Available online at www.sciencedirect.com
ScienceDirect
Journal of the European Ceramic Society 29 (2009) 1371–1377
www.elsevier.com/locate/jeurceramsoc

Suppression of grain growth in sub-micrometer alumina via two-step sintering method

Z. Razavi Hesabi [a,*], M. Haghighatzadeh [a], Mehdi Mazaheri [a,*], Dusan Galusek [b], S.K. Sadrnezhaad [a,c]

[a] *Materials and Energy Research Center (MERC), P.O. Box 14155-4777, Tehran, Iran*
[b] *Vitrum Laugaricio-Joint Glass Centre of IIC SAS, TnU AD and RONA, j.s.c., Trencin, Slovak Republic*
[c] *Center of Excellence for Production of Advanced Materials, Department of Materials Science and Engineering, Sharif University of Technology, P.O. Box 11365-9466, Tehran, Iran*

Received 13 April 2008; received in revised form 21 August 2008; accepted 27 August 2008
Available online 11 October 2008

Abstract

Two-step sintering (TSS) was applied to suppress the accelerated grain growth of sub-micron (∼150 nm) alumina powder. The application of an optimum TSS regime led to a remarkable decrease of grain size down to ∼500 nm; while the grain size of the full-dense structures produced by conventional sintering ranged between 1 and 2 μm. To find how important the temperatures at sintering steps might be, several TSS regimes were conducted. The results showed that the temperatures at both sintering steps play vital roles in densification and grain growth of the alumina compacts. Based on the results, the optimum regime consisted of heating the green bodies up to 1250 °C (first step) and then holding at 1150 °C for more than 60 h (second step). This yielded the finest microstructure with no deterioration of the densification. Heating at 1300 °C (first step) and then at 1200 °C (second step) was not a successful procedure. Lowering the temperature of the second step down to 1100 °C resulted in exhaustion of the densification at 88% -theoretical density. A nearly full-dense structure with an average grain size of 850 nm was obtained when the temperature of the second step was increased to 1150 °C. Empirical results show that not only the first step temperature has to be high enough to reach a structure containing unstable pores, but the second sintering temperature must also be high enough to activate the densification mechanism without grain growth. This means that a considerable densification at the first step does not imply enough second-step densification.

Keywords: Al_2O_3; Sintering; Grain growth

1. Introduction

Large increase in strength and hardness is frequently documented for ultra-fine ceramic/metallic structures; a phenomenon that is explained in part by small grain sizes using the well-known Hall–Petch relationship.[1–4] Difficulties are associated with producing ultra-fine bulk structures[5–7] due to the fact that fine structures with high interface density must store relatively high energies. As a consequence, grain refining processes have attracted much attention recently.[8,9] To achieve this goal, two principal ways are applied: decreasing the grain size from microscale down to ultra-fine range (<300 nm) and inhibiting the growth of ultra-fine grains during processing. The former has been usually used to produce ultra-fine metallic materials, while the latter has most often been conducted to obtain ultra-fine ceramics. Langdon et al.[10,11] have, for instance, refined the structure of aluminum alloys via severe plastic deformation through equal channel angular pressing (ECAP). Large plasticity of metals and alloys -allows them to be severely deformed, while the brittle nature of ceramics restricts the applicability of this method. In order to obtain an ultra-fine ceramic structure, one can use nanocrystalline powder. Accelerated grain growth during final stage of sintering usually results, however, in coarsening of the structure. Although the higher surface area of powders provides higher driving force and promotes densification leading to a decrease of interfacial energy, it increases their tendency to form agglomerates.[12,13] Dry pressing of the agglomerated powders leads to the formation of a green body with

* Corresponding authors. Tel.: +98 9121365786/+41 21 693 3389; fax: +41 21 693 4470.
E-mail addresses: zohreh.razavi@gmail.com (Z. Razavi Hesabi), mehdi.mazaheri@epfl.ch, mmazaheri@gmail.com (M. Mazaheri).

0955-2219/$ – see front matter © 2008 Elsevier Ltd. All rights reserved.
doi:10.1016/j.jeurceramsoc.2008.08.027

two types of pores in this case: micrometric inter-agglomerate pores, which degrade densification, coexisting with nanometric inter-crystalline pores. During sintering, the elimination of the inter-agglomerate pores requires high temperatures promoting grain growth which is incompatible with keeping the sintered grain size in the nanometer range.[13] To overcome this difficulty, loosely agglomerated larger particles could be used as the starting powder. Krell et al.[14] reports the preparation of ultra-fine sintered bodies from sub-micron powders rather than from nanometer-sized ones. If such coarser powders are shaped in a proper way, not only does the sintering temperature decrease but also the grain growth would be minimized due to smaller and more homogenously distributed pores in a green body with higher green density. Dense structures with fine grain size and improved mechanical properties would, hence, be producible.[3,14,15]

To preserve fine grains while sintering, a second phase could be added to pin grain boundaries. For instance, Chen et al.[16] prohibited grain growth of nanocrystalline zirconia with doping TiO_2 particles. In doing so, a homogenous distribution of the second phase is needed. The size of the second phase as well as the type and its thermal stability drastically influence the drag pinning force and the final grain size.[17,18] The results of Bernard-Granger and Guizard[17] showed that the influence of TiO_2 in suppression of grain growth in sub-micrometer alumina was not considerable while a significantly smaller grain size was obtained by addition of MgO particles. Chakravarty et al.[18] reported that with increasing of MgO content above 1.25 wt.%, densification of sub-micron Al_2O_3 was retarded. Moreover, it is not easy to achieve a good distribution of fine second phase in nanopowders to prohibit grain growth. Another way to hamper grain growth is the utilization of pore pinning during densification.[19] In other words, instead of the second phase, one can use pores to inhibit grain growth. Novikov[19] simulated the grain growth in a three-dimensional microstructure while dispersed particles like sintering pores move with boundaries reducing the rate of the grain growth.

From the thermodynamics aspect, at a temperature range where grain boundary diffusion is active, but grain boundary migration is sufficiently sluggish, densification would continue without any significant grain growth. On basis of this idea, Chen and Wang[20] developed a novel technique called two-step sintering (TSS) to suppress the accelerated grain growth at the final stage of sintering by triple junctions. To take the advantage of boundary dragging by triple junctions, a critical density at first should be achieved where sufficient triple junctions exist throughout the body as pins. Then with decreasing the sintering temperature to a critical degree, the grain growth would be stopped by triple junctions while densification may not be impaired. In doing so, samples have to be exposed to prolonged isothermal heating at the second (low temperature) step. Referring to the conducted successful TSS in open literature, different critical densities were reported for various systems. For instance, Chen and Wang[20] determined 75% of the theoretical density (TD) as the critical one for TSS of nano-yttria to succeed. Li and Ye[21] reported that below 82% TD, alumina nanopowder would not be densified even after prolong soaking in the second step. As in a TSS regime, the triple junctions are going to prohibit grain growth, while unstable pores can shrink with low temperature annealing, seemingly the source of different densities lies in the pore size and distribution which needs to be further investigated. Certainly, formation of inhomogeneous porosity due to the increased tendency of nanopowder to form agglomerates complicates the situation. To solve this problem, one can use larger particles with lower agglomeration degree and shape green bodies with advanced methods to obtain a more homogenous structure. Under this condition, one can expect successful TSS at lower temperatures.

In the present study, TSS was applied to the sub-micrometer Al_2O_3 powders to achieve a dense ultra-fine structure. The sintering behavior and structural evolution during densification were traced to find out the densification mechanism. The effect of temperature of both sintering steps on densification and grain growth at different TSS regimes were discussed. Hardness and fracture toughness of the two-step sintered samples were also reported.

2. Experimental procedure

2.1. Raw materials and compaction

Alumina powder (Taimicron TM-DAR; Taimei Chemicals Co., Ltd., Tokyo, Japan) with a mean particle size of 150 nm was used. The morphology of powder was examined with a scanning electron microscope (SEM, Philips XL30, the Netherlands). The powder was firstly shaped in a cylindrical die with 10 mm diameter under uniaxial pressure of 50 MPa. The preformed green samples were then cold isostatic pressed under 200 MPa.

2.2. Porosimetery

To estimate how the two shaping methods of cold isostatic pressing (CIP) and uniaxial pressing (UP) would influence on sintering (densification and grain growth) and pore size distribution of samples shaped through CIP and UP (at 100 MPa) mercury porosimetry tests were also conducted on pre-sintered/sintered samples at 1100, 1300 and 1350 °C without isothermal dwell.

2.3. Sintering

Both conventional sintering (CS) and TSS of the green bodies shaped through CIP were carried out in this research. CS specimens were non-isothermally sintered between 1050 and 1400 °C in air with a heating ramp of 10 °C min^{-1}. Different TSS regimes were applied to minimize the final grain size. At the first step, pellets were heated up to T_1 with a heating ramp of 10 °C min^{-1}. They were then cooled down to the lower temperatures of T_2 with a cooling rate of 50 °C min^{-1} and soaked for a prolonged period of time. Table 1 lists the conditions under which TSS regimes were carried out. The density of the sintered samples was measured by Archimedes method in water. To prevent penetration of water to the open pores of the sample, their surface was wax smeared. The mean diameter of the grains

Table 1
The conditions for TSS regimes

TSS regime	T_1 (°C)	T_2 (°C)	Maximum holding time at T_2 (h)
TSS1	1300	1200	15
TSS2	1300	1100	15
TSS3	1300	1150	50
TSS4	1200	1150	15
TSS5	1250	1150	64

was measured using SEM micrographs of the fractured surfaces, counting at least 150 grains for each specimen. The average of at least three measurements was reported as the final result of the tests.

2.4. Mechanical properties

Hardness and fracture toughness were measured by indentation method. Indentation tests were conducted on polished samples with a load of 10 kg held for 20 s. The hardness (H_v) was calculated from the diagonal length of the indentation determined by SEM observation using the following equation[22]:

$$H_V = \frac{1.854P}{d^2} \quad (1)$$

where P is the applied load and d is the mean value of the diagonal length. Fracture toughness (K_{IC}) was determined by measuring the crack length emanating the indentation center indicated by C in the following equation[23]:

$$K_{IC} = 0.0016\left(\frac{E}{H_V}\right)^{1/2}\left(\frac{P}{C^{3/2}}\right) \quad (2)$$

where E is the Young's modulus.

3. Results

Fig. 1 shows the SEM micrograph of the as-received sub-micrometer (150 nm) alumina powder. As seen, no tight agglomeration can be observed. Fig. 2 shows pore size distribution in green compacts shaped via uniaxial pressing as well as CIP after heating up to 1100 °C. As shown, uniaxial pressing followed by CIP shifted the mean pore size to a smaller value. As no significant densification was achieved, these curves can be considered as an indicator for pore size distribution in green state (before sintering). Fig. 3 shows the structural evolution of green compacts shaped via CIP while firing through heating up to 1400 °C with a heating rate of 10 °C min^{-1}. Up to 1250 °C, no obvious change in grain size was observed while a significant increase in density occurred. Further increase of temperature (up to 1300 °C) yielded a density of ~87% TD and a grain size of ~350 nm. Densification was; however, nearly complete (~98% TD) at 1400 °C without isothermal dwelling. Final grain size of the nearly fully dense structure was higher than 1.2 μm. In other words, 11% increase of relative fired density (from ~87 to ~98% TD) led to a remarkable grain growth of more than 240% (from ~350 nm to ~1.2 μm). To suppress the grain growth, different TSS regimes were applied to densify green compacts without the accelerated grain growth at the final stage of sintering. In doing so, long time isother-

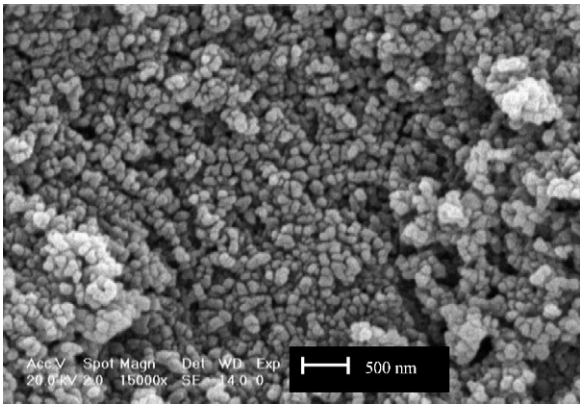

Fig. 1. SEM image of sub-micron Al_2O_3 powder.

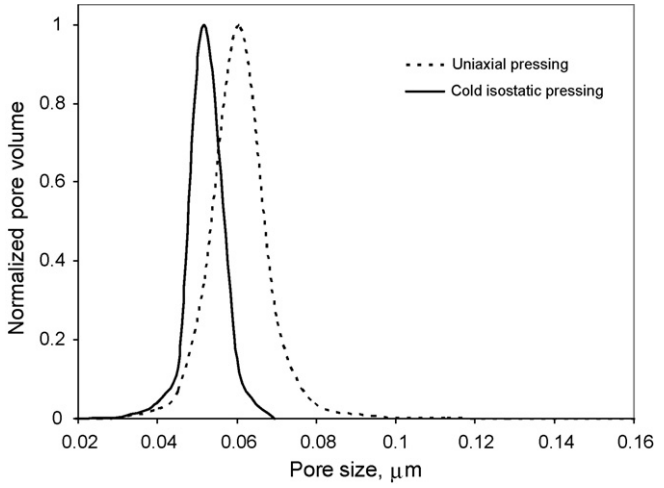

Fig. 2. Pore size distribution in pre-sintered samples shaped via uniaxial pressing and cold isostatic pressing (green samples were heated to 1100 °C with no holding).

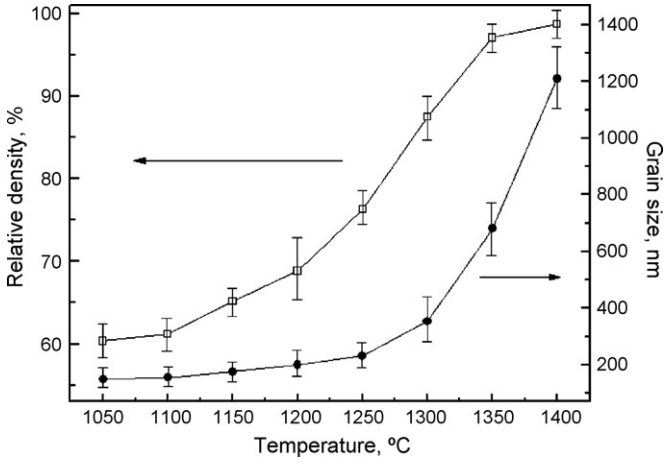

Fig. 3. Structural evolution (relative fired density and grain size) of sub-micron Al_2O_3 green compacts through heating up with a constant heating ramp of 10 °C min^{-1}.

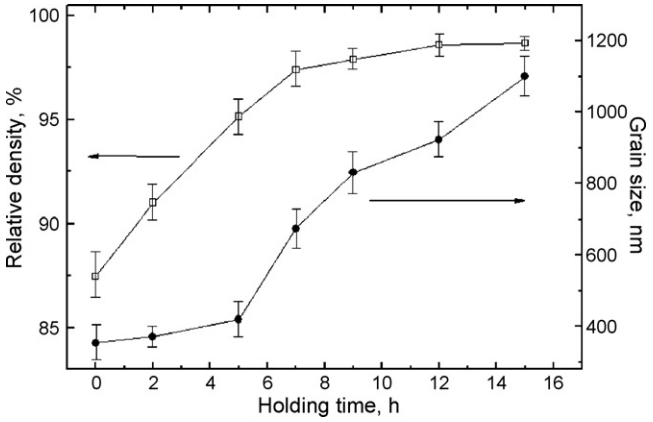

Fig. 4. Relative fired density and grain size versus holding time at 1200 °C for sub-micron Al_2O_3 green compacts firstly heated up to 1300 °C (TSS1).

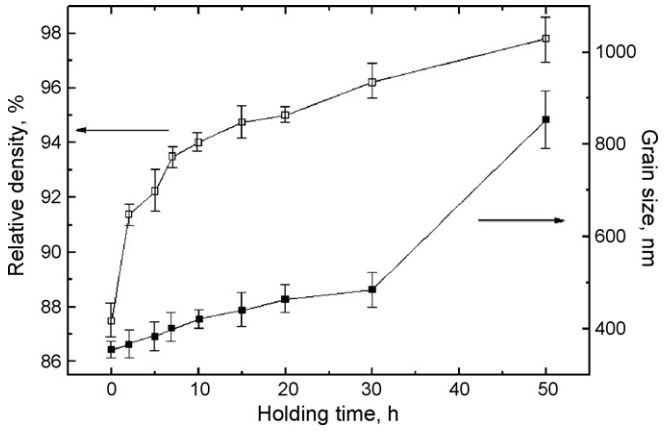

Fig. 6. Relative fired density and grain size versus holding time at 1150 °C for sub-micron Al_2O_3 green compacts firstly heated up to 1300 °C (TSS3).

mal dwell at lower temperatures instead of continuous heating up/isothermal dwell at a constant temperature were reported to be effective.[24] Fig. 4 shows the variation of relative fired density and grain size versus holding time at 1200 °C for samples firstly heated up to 1300 °C (TSS1). Although the temperature was decreased 100 °C in the second step, a significant grain growth was observed. In other words, coarse structure with an average grain size of ~1.1 μm was obtained, comparable to that achieved via continuous heating up to 1400 °C. The maximum relative density of both samples was ~98% TD. To succeed in inhibiting the grain growth, the second step temperature was decreased further to 1100 °C (TSS2). As observed in Fig. 5, even after 16 h soaking at 1100 °C only a slight increase in density was achieved. Most obviously, the second step temperature was not sufficient for elimination of the residual porosity. Figs. 4 and 5 illustrate how important the temperate of the second step might be. Not only did low temperature isothermal dwell in the second step fail to eliminate the residual porosity, but also high temperature soaking led to an uncontrolled grain growth. Seemingly, there is a critical temperature between 1100 and 1200 °C which could be chosen as the second step temperature for elimination of the residual porosity without accelerated growth of grains. Fig. 6 shows the results of the density and the grain size measurements for TSS3 cycle conducted at $T_1 = 1300$ °C and $T_2 = 1150$ °C (1100 °C < T_2 < 1200 °C). After 50 h dwell at 1150 °C, green compacts were densified and relatively finer structures with an average grain size of ~0.85 μm were obtained. To find how effective the first step temperature might be, T_1 was decreased from 1300 down to 1200 °C (TSS4). Fig. 7 shows the effect of decreasing the temperature of the first step on densification and grain growth versus holding time. With decreasing the temperature in the first step, the density (obtained at the end of the first step) was decreased from ~87.5 to ~69% TD. After 9 h soaking at 1150 °C the density increased up to ~90% TD while further soaking did not affect densification any more. The grain size was increased from ~200 to ~310 nm. The results indicate that the initial density after the first step was lower than the critical one, which resulted in failure of the procedure. To increase the initial density, the samples were heated up to 1250 °C. Fig. 8 shows structural evolution of green compacts firstly fired through heating up to 1250 °C followed by holding at 1150 °C (TSS5). Successfully, 50 °C increase of the first step temperature led to formation of a nearly full-dense structure with an average grain size of ~500 nm. The final density of sintered bodies achieved 98% TD.

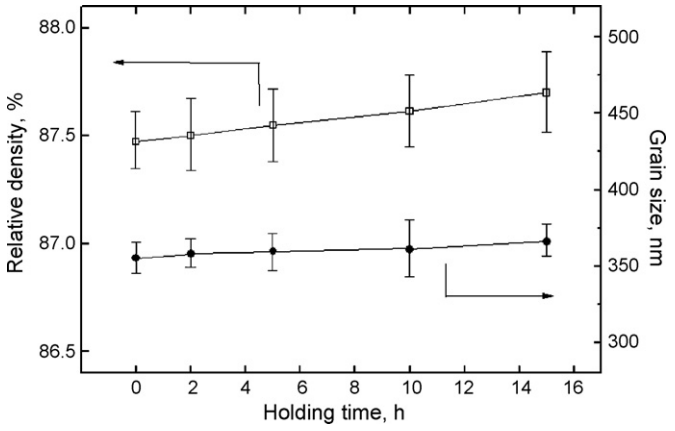

Fig. 5. Relative fired density and grain size versus holding time at 1100 °C for sub-micron Al_2O_3 green compacts firstly heated up to 1300 °C (TSS2).

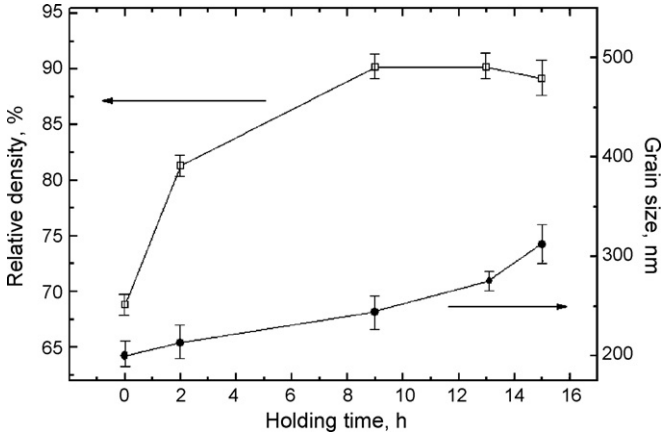

Fig. 7. Relative fired density and grain size versus holding time at 1150 °C for sub-micron Al_2O_3 green compacts firstly heated up to 1200 °C (TSS4).

4. Discussion

4.1. Densification and grain growth

4.1.1. Conventional sintering

It is needless to say that shaping method as well as powder characteristics would significantly influence the sintering path of ceramic powders.[3,12,14,15] For instance, Krell et al.[3,14,15] showed that conventional sintering of uniaxially pressed submicron alumina at 1450 °C gave a density of ~98% TD and a grain size of 1.25 μm. While uniaxial pressing, followed by CIP and subsequent sintering at 1400 °C increased the density to 99% TD and reduced the grain size to 650 nm. It was attributed to the higher homogeneity of particle coordination.[3,14,15] Similarly the results of the present study show that uniaxial pressing followed by CIP improved particle coordination. Fig. 2 indicates more homogeneous particle coordination in samples shaped through CIP in comparison with uniaxially pressed compacts, expressed in the reduction of pore size as well as narrowing of pore size distribution.

Another factor affecting green state homogeneity and consequently sintering behavior of powder is agglomeration degree. For instance, Li and Ye[21] reported that after 1 h sintering of uniaxially pressed nanopowder with a mean particle size of 10 nm at 1400 °C, the relative fired density of 82% was attainable. Although the nanometer powder with a significantly higher surface area was used, even after 1 h soaking at 1400 °C, the density is lower than that obtained in the present study without dwelling at the same temperature (~98% TD). Owing to loosely agglomerated nature of the used powder (Fig. 1), a good sinterability was observed while hard agglomerates of a 10 nm powder resulted in its significant reduction.[21] In other words, using a finer powder with higher activation energy for sintering does not guarantee better sinterability.

4.1.2. Two-step sintering

Two-step sintering tests show that there is a critical temperature for the second step as well as for the first one (Figs. 3–7). Low temperature isothermal dwelling at 1100 °C in the second step failed, for instance, to eliminate the residual porosity of samples which were firstly heated up to 1300 °C (TSS2) (see Fig. 5). High temperature soaking at 1200 °C led to an accelerated grain growth (TSS1) (Fig. 4), while with further decrease of the second temperature (T_2), the TSS was successfully conducted (TSS3) (Fig. 6). Fig. 8 shows an initial density of 75% TD is sufficient for removal of pores in the second step (TSS5). Bodisova et al.[25] observed, however, that 75% TD after the first sintering step is not sufficient in the case of the used powder and at least a density of 92% TD must be achieved before the second step. This discrepancy can be attributed to the shaping method of green compacts resulting in different mean pore size and its distributions. As seen in Fig. 2, not only the mean pore size in CIP sample is smaller than that of UP, but also a narrower pore size distribution can be observed. Accordingly, in the present study the temperature of the first step in TSS of submicron Al_2O_3 could be decreased to 1250 °C in comparison with 1400 °C of Ref. [25]. The minimum temperature necessary for the second step in both studies was 1150 °C although the relative density of the samples at the beginning of the second step was not identical. Obviously, independently of the initial density at the beginning of the second step the pore size and its distribution dictate whether or not the second sintering step could be successfully completed. Fig. 9 compares the cumulative pore size distribution curves of CIP and UP samples sintered at different temperatures. Most obviously, at all temperatures, CIP samples contain finer residual pores with narrower size distribution. These results confirm enhanced sinterability of more homogeneous CIP-ed samples. Fig. 10 shows the SEM micrograph of samples sintered under optimum TSS regime (TSS5). The average grain size of ~500 nm was achieved in this case. In comparison with the results mentioned in Ref. [25], the final grain size was decreased from 0.9 to 0.5 μm. It could be concluded that the pore size and its distribution obtained after the first step determine the critical density which guarantees the success of a TSS cycle.

Fig. 11 summarizes the effect of different TSS regimes on sintering paths of sub-micron alumina compared with that obtained

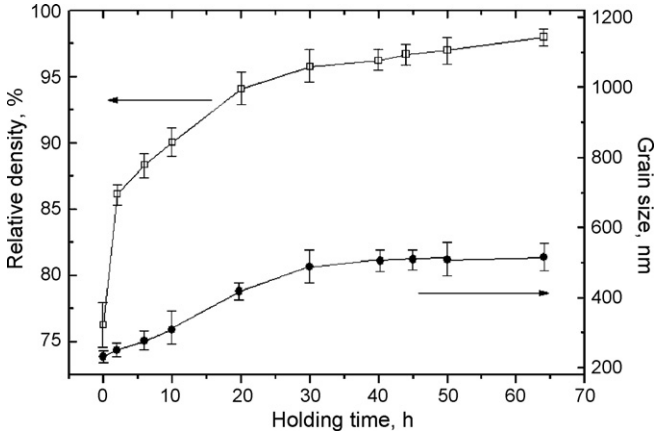

Fig. 8. Relative fired density and grain size versus holding time at 1150 °C for sub-micron Al_2O_3 green compacts firstly heated up to 1250 °C (TSS5).

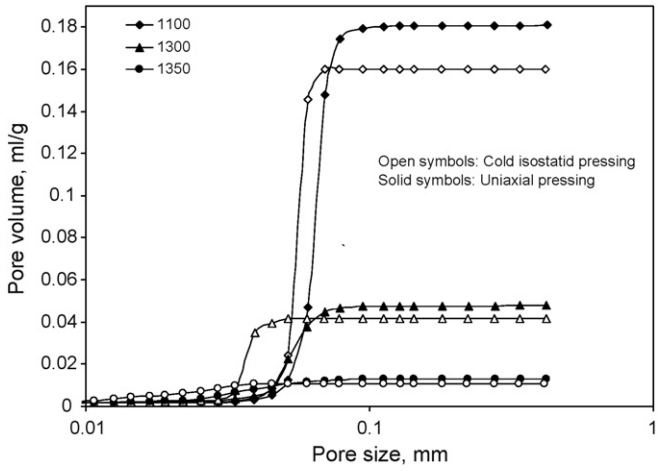

Fig. 9. Cumulative curves of pore size distribution in samples shaped via uniaxial pressing and cold isostatic pressing after heating up to 1100, 1300 and 1350 °C.

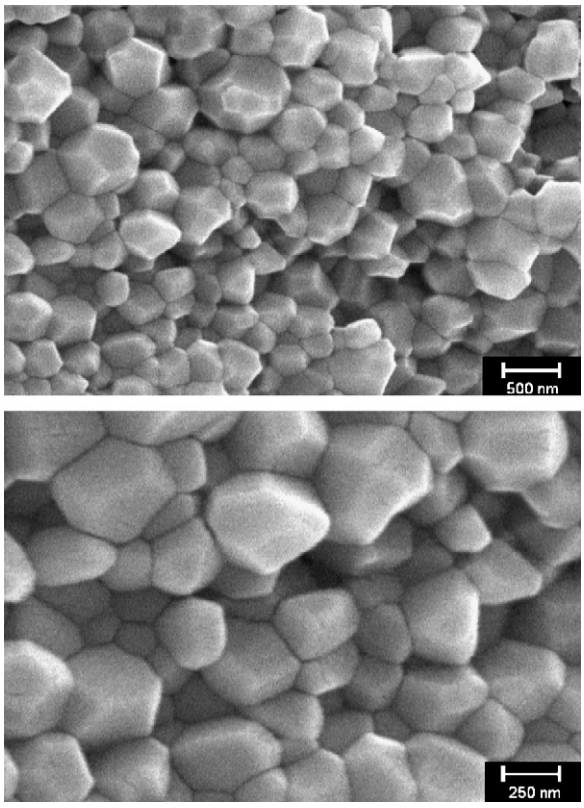

Fig. 10. SEM picture of sintered sub-micron Al_2O_3 under TSS5 regime (the green sample firstly heated up to $T_1 = 1250\,^{\circ}C$, cooled down to $T_2 = 1150\,^{\circ}C$ and held at T_2 for 64 h).

through continuous heating. It is shown how effectively the temperatures of the two sintering steps in TSS cycles affect the densification and grain growth processes.

4.2. Mechanical properties: hardness and fracture toughness

The finer the grain size of a structure is, the higher the density of grain boundaries would be. This constrains the plastic deformation of the sample during loading and attracts the engineers due to their more desirable mechanical properties. Accelerated grain growth at the final stage of sintering especially when nanocrystalline powder is used, is a big challenge in producing ultra-fine structures. To prohibit grain growth, one can sacrifice densification.[21] The residual porosity deteriorates considerably the mechanical properties such as hardness and bending strength. Table 2 summarizes the hardness and the fracture toughness of the bodies sintered under TSS3 and TSS5 with final grain size of 0.85 and 0.5 μm, respectively. In the present study, ultra-fine grained structures with desirable mechanical properties were produced via a simple pressureless sintering method that did not deteriorate densification. The fracture toughness of 4.24 ± 0.21 MPa m$^{1/2}$ is in the range of values reported in the literature.[18,26] With increasing of the grain size from 0.5 μm (TSS5) to 0.85 μm (TSS3), the hardness decreased while the indentation fracture toughness remained the same.

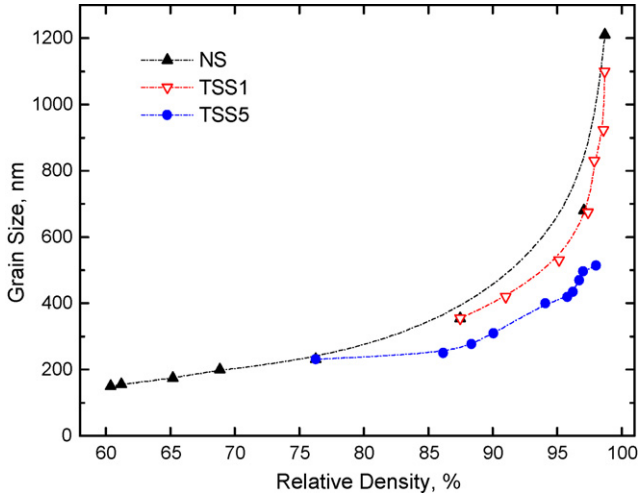

Fig. 11. Structural evolution of sub-micron Al_2O_3 green compacts through heating up to 1400 °C and different TSS heating regimes.

Table 2
Mechanical properties of sub-micron Al_2O_3 compacts sintered under TSS3 and TSS5 condition

Sintering regime	Fractional fired density (%)	Grain size (μm)	Hardness (GPa)	Fracture toughness (MPa m$^{1/2}$)
TSS3	97.8	0.85	15.01	4.29
TSS5	98	0.5	18.2	4.24

5. Conclusion

Sub-micron Al_2O_3 powder with an average particle size of 150 nm was sintered via two-step sintering (TSS) method. To obtain minimum grain size, different TSS cycles were tested. The structural evolution during sintering was traced. The results showed that low temperature isothermal dwell at 1150 °C after heating the green compacts up to 1300 °C decreased the grain size from 1.2 μm down to 850 nm. Further decrease of the first step temperature to 1250 °C led to formation of a finer structure with an average grain size of 500 nm. The hardness and fracture toughness of the samples sintered under optimum TSS regime were 18.2 ± 0.55 GPa and 4.24 ± 0.21 MPa m$^{1/2}$, respectively.

References

1. Han, B. Q., Lee, Z., Nutt, S. R., Lavernia, E. J. and Mohamed, F. A., Mechanical properties of an ultrafine-grained Al—7.5 pct Mg alloy. *Metallurgical and Materials Transactions A*, 2003, **34**, 603–613.
2. Masumura, R. A., Hazzledine, P. M. and Pande, C. S., Yield stress of fine grained materials. *Acta Materialia*, 1998, **46**, 4527–4534.
3. Krell, A. and Blank, P., The influence of shaping method on the grain size dependence of strength in dense submicrometre alumina. *Journal of the European Ceramic Society*, 1996, **16**, 1189–1200.
4. Vaben, R. and Stover, D., Processing and properties of nanophase ceramics. *Journal of Materials Processing Technology*, 1999, **92–93**, 77–84.
5. Driver, J. H., Stability of nanostructured metals and alloys. *Scripta Materialia*, 2004, **51**, 819–823.
6. Song, X., Liu, G. and Gu, N., Influence of the second-phase particle size on grain growth based on computer simulation. *Materials Science and Engineering A*, 1999, **270**, 178–182.

7. Mazaheri, M., Valefi, M., Razavi Hesabi, Z., and Sadrnezhaad, S. K., Two-step sintering of nanocrystalline $8Y_2O_3$ stabilized ZrO_2 synthesized by glycine nitrate peocess. *Ceramics International*, in press.
8. Suryanarayana, C., Mechanaical alloying and milling. *Progress in Materials Science*, 2001, **46**, 1–184.
9. Bowen, P., Carry, C., Luxembourg, D. and Hofmann, H., Colloidal processing and sintering of nanosized transition aluminas. *Powder Technology*, 2005, **157**, 100–107.
10. Langdon, T. G., The principles of grain refinement in equal-channel angular pressing. *Materials Science and Engineering A*, 2007, **462**, 3–11.
11. Xu, C., Furukawa, M., Horita, Z. and Langdon, T. G., Using ECAP to achieve grain refinement, precipitate fragmentation and high strain rate superplasticity in a spraycast aluminum alloy. *Acta Materialia*, 2003, **51**, 6139–6149.
12. Ferkel, H. and Hellmig, R. J., Effect of nanopowder deagglomeration on the densities of nanocrystalline ceramic green bodies and their sintering behavior. *Nanostructured Materials*, 1999, **11**, 617–622.
13. Bowen, P. and Carry, C., From powders to sintered pieces: forming, transformations and sintering of nanostructured ceramic oxides. *Powder Technology*, 2002, **128**, 248–255.
14. Krell, A., Blank, P., Ma, H., Hutzler, T. and Nebelung, M., Processing of high-density submicrometer Al_2O_3 for new applications. *Journal of the American Ceramic Society*, 2003, **86**, 546–553.
15. Krell, A. and Klimke, J., Effects of the homogeneity of particle coordination on solid-state sintering of transparent alumina. *Journal of the American Ceramic Society*, 2006, **89**, 1985–1992.
16. Chen, T., Tekeli, S., Dillon, R. P. and Mecartney, M. L., Phase stability, microstructural evolution and room temperature mechanical properties of TiO_2 doped 8 mol% Y_2O_3 stabiized ZrO_2 (8Y-CSZ). *Ceramics International*, 2008, **34**, 365–370.
17. Bernard-Granger, G. and Guizard, C., Influence of MgO or TiO2 doping on the sintering path and on the optical properties of a submicronic alumina material. *Scripta Materialia*, 2007, **56**, 983–986.
18. Chakravarty, D., Bysakh, S., Muraleedharan, K., Rao, T. N. and Sundaresan, R., Spark plasma sintering of magnesia-doped alumina with high hardness and fracture toughness. *Journal of the American Ceramic Society*, 2008, **91**, 203–208.
19. Novikov, V. Y., Grain growth controlled by mobile particles on grain boundaries. *Scripta Materialia*, 2006, **55**, 243–246.
20. Chen, I.-W. and Wang, X.-H., Sintering dense nanocrystalline ceramics without final-stage grain growth. *Nature*, 2000, **404**, 168–171.
21. Li, J. and Ye, Y., Densification and grain growth of Al_2O_3 nanoceramics during pressureless sintering. *Journal of the American Ceramic Society*, 2006, **89**, 139–143.
22. Tekeli, S., Fracture toughness (KIC), hardness, sintering and grain growth behavior of $8YSCZ/Al_2O_3$ composites produced by colloidal processing. *Journal of Alloys and Compounds*, 2005, **391**, 217–224.
23. Anstis, G. R., Chantikul, P., Lawn, B. R. and Marshall, D. B., A critical evaluation of indentation techniques for measuring fracture toughness. I. Direct crack measurements. *Journal of the American Ceramic Society*, 1981, **64**, 533–543.
24. Mazaheri, M., Zahedi, A. M. and Sadrnezhaad, S. K., Two-step sintering of nanocrystalline ZnO compacts: effect of temperature on densification and grain growth. *Journal of the American Ceramic Society*, 2008, **91**, 56–63.
25. Bodisova, K., Sajgalik, P., Galusek, D. and Svancare, P., Two-stage sintering of alumina with submicrometer grain size. *Journal of the American Ceramic Society*, 2007, **90**, 330–332.
26. Shen, Z., Johnsson, M., Zhao, Z. and Nygren, M., Spark plasma sintering of alumina. *Journal of the American Ceramic Society*, 2002, **85**, 1921–1927.